

ANALYTICAL COMPUTATIONAL MODELS FOR BUCKLING AND POSTBUCKLING OF THIN- WALLED STIFFENED COMPOSITE PANELS

JAKOB C. SCHILLING* AND CHRISTIAN MITTELSTEDT*

* Institute for Lightweight Construction and Design
Technical University of Darmstadt, Department of Mechanical Engineering
Otto-Berndt-Str. 2, 64287 Darmstadt, Germany
e-mail: jakob.schilling@klub.tu-darmstadt.de, web page: <https://www.klub.tu-darmstadt.de/>

Key words: Buckling, Composites, Postbuckling, Analytical, Computational model

Abstract. The loss of stability is critical in regard to thin-walled composite structures which are widespread in weight critical applications. These applications include, for example, spacecraft, aircraft and marine vessels. For the example of omega-stringer stiffened panels, the buckling and postbuckling behaviour is investigated using closed-form analytical approximate solutions. They are derived based on energy methods and their focus lies on local stability behaviour. Hereby, different load cases are included and the quality of the computational models is assessed in comparison to Lévy-type solutions or finite element analyses. The main benefit of the new models lies in their reduced computational effort compared to numerical methods. This is especially relevant in preliminary design stages, where a large number of panel configurations have to be taken into account. Thus, the new analytical computational models aid to increase the performance of thin-walled composite structures in practical applications.

1 INTRODUCTION

The stability behaviour of thin-walled structures can be analysed and described by many different methods. The range of methods that can address this type of problem reaches from purely numerical methods to closed-form analytical solutions. For optimization in preliminary design the computational effort is important as it involves the analysis of numerous different design configurations of a structural element. On the one hand numerical methods, such as the finite element method (FEM), offer flexibility to deal with various complex boundary conditions and structural elements without substantial simplification of the structural situation [1]. On the other hand the cost in terms of computational effort is still high compared to analytical methods [2]. Closed-form analytical methods are applicable to limited structural situations but are highly efficient as presented in the following for the analysis of the stability behaviour.

Other methods that are present in the range between closed-form analytical and FEM are for example the finite strip method or the Ritz-method. For brevity the reader is referred to References [3, 4] for a more detailed literature review. The present work is concerned with the analysis of the stability behaviour of thin-walled structures made

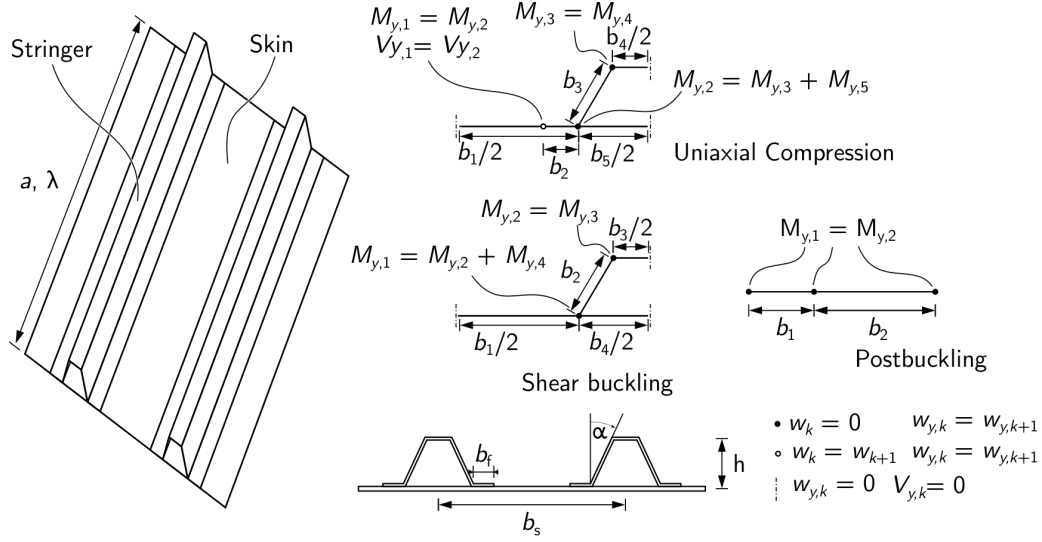


Figure 1: Omega-stringer-stiffened panels and its idealization for each loadcase or analysis type.

of composite material to address the lack of highly efficient computational models that include their complex material behaviour.

This type of structures is especially sensitive to buckling and postbuckling in the context of their application in aircraft, spacecraft, and marine vessels. A flat stiffened composite panel braced with omega stringers presented in Figure 1 is investigated with a closed-form linear local buckling analysis for two different load cases in the present work. In case of uniaxial loading the present approach is a summarized version of the detailed derivation discussed in Ref. [3] and in the case of shear loading, the derivation is presented in Ref. [4]. Solutions for both cases can be obtained following the generalized approach described in the present work. The investigation into the linear local stability behaviour is extended to the postbuckling range following the methodology of Ref. [5, 6, 7] Hereby, the omega-stringer stiffened panel is simplified as a combination of two plates of different width with periodic boundary conditions to obtain first insights into its postbuckling behaviour.

The approach presented in the following sections, starting with the local buckling analysis, is based on the classical laminated plate theory and van Kármán strains. The details of these fundamental assumptions can be found in textbooks like Ref. [5, 8, 9].

2 LOCAL BUCKLING ANALYSIS

The closed-form analytical approach is presented in a generalized form and is adapted in the following sections to an idealized model of an omega-stringer-stiffened panel for two different load cases. The approach is suited for arbitrary prismatic structures that are an assembly of laminated plates. The plates are numbered using the index k . Each plate is described using its own coordinate system with the coordinates x and y_k . The x -axes of the plates are parallel. One precondition for this approach is that the plates are infinitely long or simply supported along their transverse edges. It is based on the

Ritz-method but considers Ritz-constants that are shared within the system of plates in order to minimize their number and combines this with the requirement that not only kinematic but also dynamic boundary conditions are at least approximately fulfilled. A system of buckling shape functions is formulated in the form of Eq. (1).

$$w_k = A w_{A,k}(x, y_k) + B w_{B,k}(x, y_k) \quad (1)$$

Here, A and B are the Ritz-constants of the system of k plates. For the functions $w_{A,k}$ and $w_{B,k}$, polynomials are chosen where the geometric and material parameters c_{Aik} and c_{Bik} are determined to fulfil the boundary and interface condition of the investigated problem. The functions are presented in Eq. (2).

$$\begin{aligned} w_{Ak} &= t(x, y_k) \left(c_{A0k} \frac{y_k^4}{b_k^4} + c_{A1k} \frac{y_k^3}{b_k^3} + c_{A2k} \frac{y_k^2}{b_k^2} + c_{A3k} \frac{y_k}{b_k} + c_{A4k} \right) \\ w_{Bk} &= t(x, y_k) \left(c_{B0k} \frac{y_k^4}{b_k^4} + c_{B1k} \frac{y_k^3}{b_k^3} + c_{B2k} \frac{y_k^2}{b_k^2} + c_{B3k} \frac{y_k}{b_k} + c_{B4k} \right) \end{aligned} \quad (2)$$

The function $t(x, y_k)$ describes the component in the longitudinal direction along the x -axis. This function is chosen differently depending on the loadcase. Next the total elastic potential is obtained. In order to simplify the computation the substitute variables X_k , Y_k , Z_k are introduced for the inner potential of each plate k and U_k , V_k , W_k for the external potential, respectively. The latter depend on the loadcase. The substitute variables enable the compact formulation of the potential energy presented in Eq. (3-4).

$$\Pi_{i,k} = A^2 X_k + A B Y_k + B^2 Z_k \quad (3)$$

$$\Pi_{e,k} = A^2 N_{cr} U_k + A B N_{cr} V_k + B^2 N_{cr} W_k \quad (4)$$

For the definition of the variables X_k , Y_k , and Z_k the reader is referred to Ref. [4].

The total elastic potential of the plate assembly is obtained by the summation of all individual contributions. The total number of plates is denoted with K .

$$\begin{aligned} \Pi &= \sum_{k=1}^K (\Pi_{i,k} + \Pi_{e,k}) = A^2 \left(\sum_{k=1}^K X_k + N_{cr} \sum_{k=1}^K U_k \right) \\ &+ A B \left(\sum_{k=1}^K Y_k + N_{cr} \sum_{k=1}^K V_k \right) + B^2 \left(\sum_{k=1}^K Z_k + N_{cr} \sum_{k=1}^K W_k \right) \end{aligned} \quad (5)$$

This is again simplified by introducing suitable substitute variables $\Gamma_{1,2,3}$ and $\alpha_{1,2,3}$. The fully defined elastic potential is consequently given as shown in Eq. (6).

$$\Pi = (\Gamma_1 + \alpha_1 N_{cr}) A^2 + (\Gamma_3 + \alpha_3 N_{cr}) A B + (\Gamma_2 + \alpha_2 N_{cr}) B^2 \quad (6)$$

The Ritz-method leads to two separate Ritz-equations that can be represented as linear system of equations. The buckling condition is now the vanishing of the coefficient matrix determinant of the linear system of equations. The explicit solution for the critical buckling load is easily obtained (Eq. (7)).

$$N_{\text{cr}} = \pm \frac{\Psi_2 + \sqrt{\Psi_2^2 - 4 \Psi_1 \Psi_3}}{2 \Psi_1} \quad \text{with} \quad \begin{aligned} \Psi_1 &= 4 \alpha_1 \alpha_2 - \alpha_3^2 \\ \Psi_2 &= 4 \Gamma_1 \alpha_2 + 4 \Gamma_2 \alpha_1 - 2 \Gamma_3 \alpha_3 \\ \Psi_3 &= 4 \Gamma_1 \Gamma_2 - \Gamma_3^2 \end{aligned} \quad (7)$$

The critical load N_{cr} represents either the critical uniaxial compression or shear load applied to the assembly.

2.1 Local buckling of omega-stringer-stiffened panel under uniaxial compression

The function $t(x, y_k)$ for the loadcase of uniaxial compression is presented in Eq. (8). It fulfils the simply supported boundary conditions along the loaded edges. The model is also only valid for cross-ply laminates.

$$t(x, y_k) = \sin\left(\frac{\pi m x}{a}\right) \quad (8)$$

The idealized mode of the omega-stringer-stiffened panel consists of five plates and considers symmetry conditions, as shown in Figure 1. The indicated boundary and interface conditions are the basis for the derivation of the constants c_{Aik} and c_{Bik} . The constants c_{A0k} and c_{B0k} are chosen to include the Ritz-constants in a feasible way. In the current case they are chosen as follows in Eq. (9).

$$c_{A0k} = [1, 0, 0, 0, 0] \quad c_{B0k} = [0, 1, 0, 0, 0] \quad (9)$$

The substitute variables U_k , V_k , and W_k are determined in the case of uniaxial compression as presented in Ref. [3].

The given details complete the general approach for the closed-form analytical approximate model for the description of the linear local buckling behaviour of omega-stringer-stiffened panels. For a more detailed derivation the reader is again referred to Reference [3]. In this publication, more detailed studies are shown that show the quality of the approach. In the present work only a exemplary study is discussed in the following section.

To give an impression about the quality of the present approach a study of the critical buckling load versus the aspect ratio a/b_s for different stringer spacings $b_s = b_1 + b_5$ is shown in Figure 2. For increasing stringer spacing the buckling load is reduced, which can be expected since the stringer dimensions are not changed and the thin-walled structure is weakened in regard of its stability behaviour. The results show that the closed-form analytical solution is in excellent agreement with the Lévy-type solution for the chosen material and panel dimensions. Hence, it provides an accurate and highly efficient method for the analysis of the local buckling behaviour. The difficult evaluation of the implicit Lévy solution can be avoided.

2.2 Local buckling of omega-stringer-stiffened panel under shear loading

For the analysis of the shear buckling of omega-stringer stiffened panels a different function $t(x, y_k)$ is chosen. The function is successfully introduced in Ref. [10] to adjust

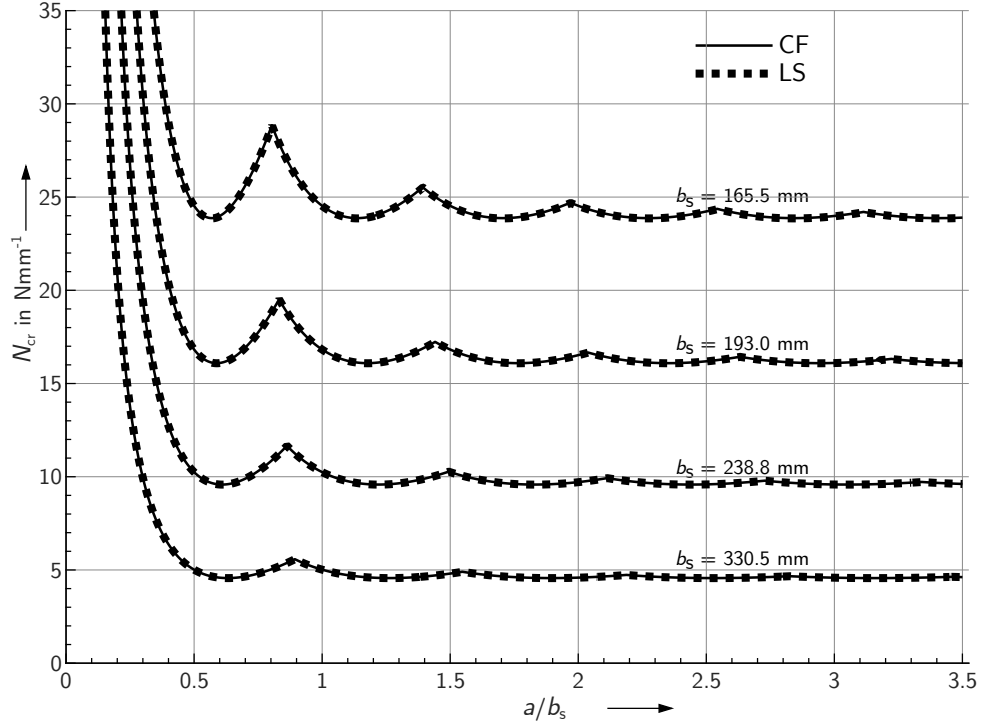


Figure 2: Buckling curves obtained with the present closed-form analytical approach (CF) [3] and the exact Lévy solution (LS) [3] for different stringer spacings b_s ; $h = 30$ mm; $\alpha = 25^\circ$; $b_2 = 0.1 b_1$; $b_5 = 55.5$ mm; stringer lay-up $[0^\circ 90^\circ 0^\circ 90^\circ 0^\circ 90^\circ 0^\circ]$; skin lay-up $[0^\circ 90^\circ 0^\circ 90^\circ]_s$; $E_1 = 150000$ MPa; $E_2 = 9000$ MPa; $G_{12} = 5300$ MPa; $\nu_{12} = 0.33$; $t_{ply} = 0.125$ mm; mod. [3]

the buckling shape functions to the oblique buckling pattern of infinitely long shear loaded plates. Instead of the panel length a , the half-wave length λ is used to describe the modes in the longitudinal direction. Furthermore, the parameters k_k are describing the obliqueness of the pattern (Eq. (10)).

$$t(x, y_k) = \sin\left(\frac{\pi}{\lambda}(x - k_k y_k)\right) \quad (10)$$

The constants c_{Aik} and c_{Bik} are similarly obtained as in the case of uniaxial compression. The idealized model with indicated boundary conditions is given in Figure 1. Note that there are only four plates in this assembly as the influence of the stringer feet is incorporated in a different way detailed in Ref. [4]. Again, the constants c_{A0k} and c_{B0k} are chosen to include the Ritz-constants (Eq. (11)).

$$c_{A0k} = [1, 0, 0, 0] \quad c_{B0k} = [0, 0, 0, 1] \quad (11)$$

The substitute variables U_k , V_k , and W_k are obtained as described in Ref. [4].

This completes the overview of the derivation. However, the solution obtained in the case of shear load is more difficult to evaluate. The critical buckling load needs to be minimized in regard of the half-wave length λ and the obliqueness parameters k_k which is easily executed using standard optimization algorithms. A very detailed description of

the derivation is available in Ref. [4] where also very extensive studies are presented and discussed. A first impression of the results is given in the following section.

The results presented in Figure 3 are obtained for a quasi-isotropic laminate and an omega stringer of varying size. The stringer spacing is kept constant for each member

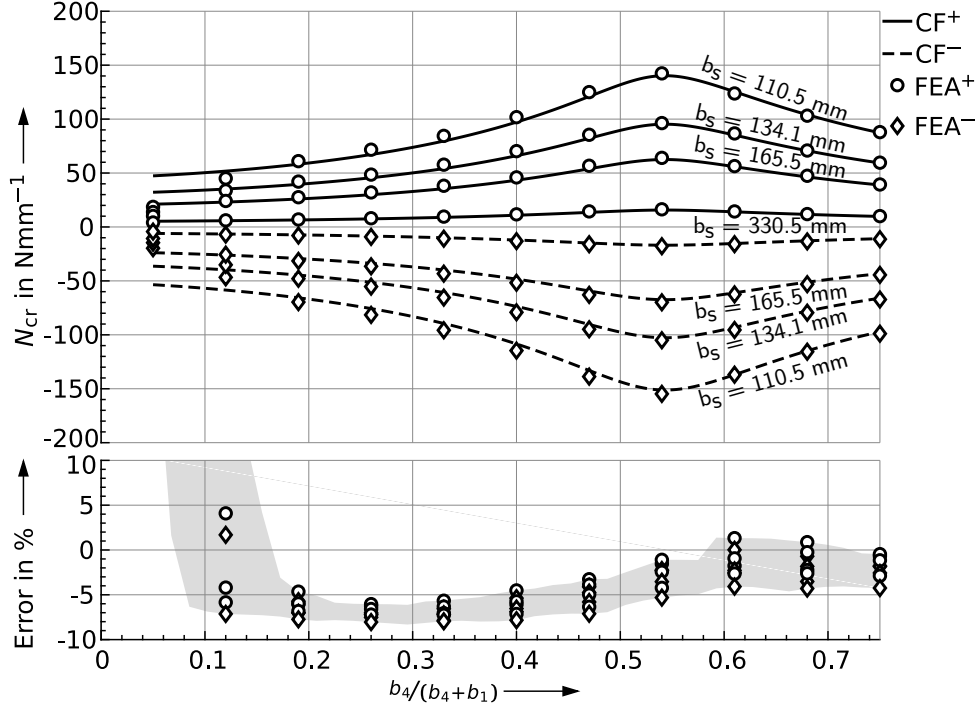


Figure 3: Effects of the scaling of the omega stringer on critical shear buckling load; positive and negative critical shear loads and errors in percent are given for the closed-form analytical model (CF) [4] and finite element analysis (FEA) [4]; $a/b_s = 3.5$; $h/b_s = 30/55.5$ mm; $\alpha = 25^\circ$; $b_f = 0.1 b_1$; stringer lay-up $[45^\circ 0^\circ - 45^\circ 0^\circ - 45^\circ 0^\circ 45^\circ]$ skin lay-up $[90^\circ 0^\circ - 45^\circ 45^\circ]_s$; $E_1 = 150000$ MPa; $E_2 = 9000$ MPa; $G_{12} = 5300$ MPa; $\nu_{12} = 0.33$; $t_{ply} = 0.125$ mm

of the family of curves. Below the results for negative and positive shear loads, the deviation is scattered in percent relative to a performed FEA analysis. The area enclosed by the limiting curves of the error is shaded in grey. In the area that is governed by local buckling ($b_4/b_4+b_1 \leq 0.2$), the results are in good agreement and show mostly a conservative approximation of the critical shear loads. This is substantiated with the given error plots. The error ranges from about -8 % to about 2 %. The shear load reaches highest absolute values when the bay plate and the stringer floor show equal buckling resistance. This impression of the results, that can be obtained using the closed-form analytical approach, indicates its applicability and the potential in reducing the computational effort for the analysis of the stability behaviour.

3 LOCAL POSTBUCKLING ANALYSIS

The analysis of the postbuckling behaviour of omega-stringer-stiffened panels is simplified in the present work. It is idealized as assembly of two plates that could also con-

servatively represent unequally stiffened panels with open cross-sectional stiffeners with periodic boundary conditions. As the postbuckling analysis is more complex than the description of the linearized problem, the modelling of the full assembly of the stiffened panel is to be discussed in future work.

The system of three differential equations per plate is reduced to a system of two introducing an individual Airy stress function ψ_k for each plate (Eq. (12)) and inverting the constitutive law.

$$N_{xx} = \psi_{k,yy}(y, x), \quad N_{yy} = \psi_{k,xx}(y, x), \quad N_{xy} = -\psi_{k,xy}(y, x) \quad (12)$$

The first remaining differential equations describes the equilibrium state of the plate (Eq (13)). Because initial imperfections are included in the analysis, the deflection w_k is substituted with $w_{0k} + w_{ik}$. The first part w_{0k} is the variable deflection and the second part w_{ik} the initial imperfection.

$$D_{11} w_{0k,xxxx} + D_{22} w_{0k,y_k y_k y_k y_k} + (2 D_{12} + 4 D_{66}) w_{0k,xy_k y_k} - (w_{0k,xx} + w_{ik,xx}) \psi_{k,y_k y_k} + 2 (w_{0k,xy_k} + w_{ik,xy_k}) \psi_{k,xy_k} - (w_{0k,y_k y_k} + w_{ik,y_k y_k}) \psi_{k,xx} = 0 \quad (13)$$

and the second the compatibility of the in-plane strains expressed with the inverted extensional stiffnesses \bar{A}_{11} , \bar{A}_{22} , and \bar{A}_{66} (Eq. 14).

$$\bar{A}_{22} \psi_{k,xxxx} + (2 \bar{A}_{12} + \bar{A}_{66}) \psi_{k,xy_k y_k} + \bar{A}_{11} \psi_{k,y_k y_k y_k y_k} = (w_{0,xy})^2 - w_{0k,xx} w_{0k,y_k y_k} - w_{0k,xx} w_{ik,y_k y_k} + 2 w_{0,xy} w_{ik,xy_k} - w_{ik,xx} w_{0k,y_k y_k} \quad (14)$$

The shape functions for the postbuckling deformation are retained from a buckling analysis following the approach in Sections 2 and 2.1 (Eq. (15)).

$$w_{k,0} = A_0 w_{A,k}(x, y_k) + B_0 w_{B,k}(x, y_k) \quad (15)$$

$$w_{k,i} = A_i w_{A,k}(x, y_k) + B_i w_{B,k}(x, y_k)$$

Also, the relationship between the amplitudes of the plates is needed for the following analysis. The amplitude scaling factor $\delta_{B/A}$ is expressed in Eq. (16).

$$\delta_{B/A} = \frac{B}{A} = -\frac{(2\Gamma_1 + 2N_{cr} \alpha_1)}{(\Gamma_3 + N_{cr} \alpha_3)} \quad (16)$$

3.1 Definition of Airy stress functions

The approach starts with the definition of Airy stress functions that fulfil the in-plane compatibility conditions. They can be split into a homogeneous solutions $\psi_{h,1,k}$ and $\psi_{h,2,k}$ and a particular solution $\psi_{p,k}$.

$$\psi_k = \psi_{h,1,k} + \psi_{h,2,k} + \psi_{p,k} \quad (17)$$

Particular solution For the particular solution, the right hand side of the compatibility equation is examined (Eq. (14)). The simplified expressions for the postbuckling shape functions (Eq. (15)) are inserted and the resulting expression is sorted and rewritten by introducing the substitute variables δ_{1k} , δ_{2k} and δ_{3k} .

$$\begin{aligned} & (w_{0,xy})^2 - w_{0k,xx}w_{0k,y_ky_k} - w_{0k,xx}w_{ik,y_ky_k} + 2w_{0,xy}w_{ik,xy_k} - w_{ik,xx}w_{0k,y_ky_k} = \\ & = (A_0^2 + 2A_0A_i)\delta_{1k} + (A_0B_0 + A_0B_i + A_iB_0)\delta_{2k} + (B_0^2 + 2B_0B_i)\delta_{3k} \end{aligned} \quad (18)$$

The functions δ_{lk} are of the following form, where $O_{1,l,k}(y_k)$ and $O_{2,l,k}(y_k)$ are polynomials of various degrees in y_k .

$$\delta_{lk} = \cos\left(\frac{2\pi m x}{a}\right) [O_{1,l,k}(y_k)] + [O_{2,l,k}(y_k)] \quad (19)$$

To obtain the particular solution $\psi_{p,k}$ for the Airy stress function, the left hand side of the compatibility equation has to match the right hand side.

$$\begin{aligned} & \bar{A}_{22}\psi_{pk,xxxx} + (2\bar{A}_{12} + \bar{A}_{66})\psi_{pk,xy_ky_k} + \bar{A}_{11}\psi_{pk,y_ky_ky_ky_k} = \\ & = (A_0^2 + 2A_0A_i)\delta_{1k} + (A_0B_0 + A_0B_i + A_iB_0)\delta_{2k} + (B_0^2 + 2B_0B_i)\delta_{3k} \end{aligned} \quad (20)$$

To achieve this the particular solution is assumed as follows.

$$\psi_{p,k} = (A_0^2 + 2A_0A_i)\omega_{1k} + (A_0B_0 + A_0B_i + A_iB_0)\omega_{2k} + (B_0^2 + 2B_0B_i)\omega_{3k} \quad (21)$$

The quantities ω_1 , ω_2 and ω_3 are undetermined functions. They have to be defined in the next step. For each plate they are of the following form (Eq. (22)).

$$\omega_{lk} = \cos\left(\frac{2\pi m x}{a}\right) \left[\sum_{n=0}^{D_{1,l,k}} F_{l,n+1,k} y_k^n \right] + \left[\sum_{n=0}^{D_{2,l,k}} F_{l,D_{1,l,k}+n+2,k} y_k^{n+4} \right] \quad (22)$$

Here, $D_{1,l,k} = \deg(O_{1,l,k})$ and $D_{2,l,k} = \deg(O_{2,l,k})$. Now, the left hand side of the compatibility equation is evaluated. This can be done for each term of $\psi_{p,k}$ separately because the aim is a comparison of the coefficients of y_k (Eq. (23)).

$$\bar{A}_{22}\omega_{lk,xxxx} + (2\bar{A}_{12} + \bar{A}_{66})\omega_{lk,xy_ky_k} + \bar{A}_{11}\omega_{lk,y_ky_ky_ky_k} = \delta_{lk}(x, y_k) \quad (23)$$

The terms $(A_0^2 + 2A_0A_i)$, $(A_0B_0 + A_0B_i + A_iB_0)$ and $(B_0^2 + 2B_0B_i)$ can be omitted as they are also present in the ansatz for $\psi_{p,k}$. Therefore, the fully defined $\omega_{l,k}$ are independent of A_0 , A_i , B_0 and B_i . With a comparison of coefficients the polynomial coefficients $F_{l,n+1,k}$ and $F_{l,\deg(O_{1,l,k})+n+2,k}$ are determined.

With the fully defined particular solution, the homogeneous solution can be obtained, subsequently.

Homogeneous solution The homogeneous solution is obtained as the solution to the homogeneous part of the differential equation describing the compatibility of the in-plane strains.

$$\bar{A}_{22} \psi_{hk,xxxx} + (2\bar{A}_{12} + \bar{A}_{66}) \psi_{hk,xy_k y_k} + \bar{A}_{11} \psi_{hk,y_k y_k y_k y_k} = 0 \quad (24)$$

The homogeneous differential equation can be solved by an exponential approach (See Ref. [6]). The first part of the homogeneous solution is redefined as follows.

$$\begin{aligned} \psi_{h,1,k}(x, y_k) = \cos\left(\frac{2\pi m x}{a}\right) & (C_{1,k} \cosh(\lambda_{1,k} y_k) + C_{2,k} \sinh(\lambda_{1,k} y_k)) \\ & + C_{3,k} \cosh(\lambda_{2,k} y_k) + C_{4,k} \sinh(\lambda_{2,k} y_k) \end{aligned} \quad (25)$$

with

$$\lambda_{1,2,k} = -\frac{\pi \sqrt{2} m \sqrt{2\bar{A}_{12,k} + \bar{A}_{66,k} \pm \sqrt{4(\bar{A}_{12,k}^2 + \bar{A}_{12,k}\bar{A}_{66,k} - \bar{A}_{11,k}\bar{A}_{22,k}) + \bar{A}_{66,k}^2}}}{\sqrt{\bar{A}_{11,k}} a} \quad (26)$$

The second part of the homogeneous solution is responsible for the constant share of the uniaxial compression acting on the plates (Eq. (27)).

$$\psi_{h,2,k}(x, y_k) = \frac{y_k^2}{b_k^2} (C_{5,k} + C_{6,k}) \quad C_{6,k} = \frac{\bar{A}_{11,2}}{2\bar{A}_{11,k}} N_{xx} b_k^2 \quad (27)$$

In-plane boundary conditions The Airy stress functions ψ_k are now complete except for the unknown constants $C_{g,k}$ for $g = 1, 2, 3, \dots, 5$. The remaining unknowns are determined by using additional in-plane boundary conditions. For the present problem, three different in-plane quantities are considered. The in plane shear forces are assumed to vanish along longitudinal edges which are also required to remain straight. This is achieved by the requirement that $v(x, y_k = \pm \frac{b_k}{2}) = \text{const}$. The boundary conditions are presented in Eq. (28).

$$N_{xy}\left(x, y_k = \pm \frac{b_k}{2}\right) = 0 \quad \frac{\partial v}{\partial x} = 0 \quad (28)$$

Finally, the equilibrium of the uniaxial loading has to be ensured by requiring that one plate of the assembly fulfils Eq. (29). In the present case $k = 2$.

$$\int_0^a \int_{-\frac{b_k}{2}}^{\frac{b_k}{2}} \frac{\partial^2}{\partial y_k^2} \psi_k(x, y_k) dy_k dx = \int_0^a \int_{-\frac{b_k}{2}}^{\frac{b_k}{2}} N_{xx} dy_k dx \quad (29)$$

The other plates are loaded by requiring that the mean displacement $u_{m,k}$ is equal.

$$u_{m,1} = u_{m,k} \quad u_{m,k} = \frac{1}{b_k} \int_{-\frac{b_k}{2}}^{\frac{b_k}{2}} \int_0^a u_{x,k}(x, y_k) dx dy \quad (30)$$

By evaluating the boundary conditions a linear system of equations is obtained which determines the constants $C_{g,k}$. They are independent of the amplitudes A_0 , A_i , B_0 and B_i .

3.2 Postbuckling amplitude with Ritz-method

The solution for the amplitude A_0 is obtained utilizing the Ritz-method. The total elastic potential is acquired by computing the internal and external contributions.

$$\Pi_{i,k} = \frac{1}{2} \int_0^a \int_{-\frac{b_k}{2}}^{\frac{b_k}{2}} \left\{ \bar{A}_{22} (\psi_{k,xx})^2 + \bar{A}_{66} (\psi_{k,xy_k})^2 + \bar{A}_{11} (\psi_{k,y_k y_k})^2 + 2 \bar{A}_{12} \psi_{k,xx} \psi_{k,y_k y_k} \right. \\ \left. + D_{11} (w_{0k,xx})^2 + 4 D_{66} (w_{0k,xy_k})^2 + D_{22} (w_{0k,y_k y_k})^2 + 2 D_{12} w_{0k,xx} w_{0k,y_k y_k} \right\} dx dy \quad (31)$$

$$\Pi_{e,k} = -N_{xx} \int_0^a \int_{-\frac{b_k}{2}}^{\frac{b_k}{2}} \left\{ \bar{A}_{12} \psi_{k,xx} + \bar{A}_{11} \psi_{k,y_k y_k} - \frac{1}{2} (w_{0k,x})^2 - w_{ik,x} w_{0k,x} \right\} dx dy \quad (32)$$

The contributions of all plates are summed up:

$$\Pi = \sum_{k=1}^2 \{\Pi_{i,k} + \Pi_{e,k}\} \quad (33)$$

After the partial derivation $\partial \Pi / \partial A$ the amplitudes B_0 and B_i are substituted with $\delta_{B/A} A_0$ and $\delta_{B/A} A_i$, respectively. Finally, the expressions are rewritten by introducing substitute variables L_1 , L_2 , L_3 , L_4 , and L_5 that are independent of A_0 , A_i , B_0 and B_i . Eq. (34) can be solved for the postbuckling amplitude.

$$A_0^3 L_1 + A_0^2 A_i L_2 + A_0 A_i^2 L_3 + A_0 L_4 + A_i L_5 = 0 \quad (34)$$

3.3 Results

Results are obtained for an exemplary panel. Note that the results are limited by the condition that $b_1 \leq b_2$ and that the used composite material is a cross-ply laminate. The in-plane load (negative in compression) is evaluated versus the deflection w for maximum values. The deflection slowly increases due to the imperfection until the critical buckling load is reached. At this point the deflection increases rapidly. Two configurations are presented. In the first both plates are of equal width and thus yield identical deflections. The are in very good agreement with the FEM. Also, the configuration of a small plate 1 that is 25 % of the width of plate 2 yields very good agreement. Only slight deviations for higher load proportionality factors are noticeable. Thus, the present approach represents a promising first step in the analysis of a full assembly of an omega-stringer-stiffened panel with periodic boundary conditions. The current model needs to be extended to be capable of dealing with at least four different plates.

4 CONCLUSIONS

- The presented formulation of the closed-form analytical solution of the stability problem of thin-walled structures shows that it can be presented in a generalized fashion that can be applied to prismatic structures in order to investigate their local buckling and postbuckling behaviour.

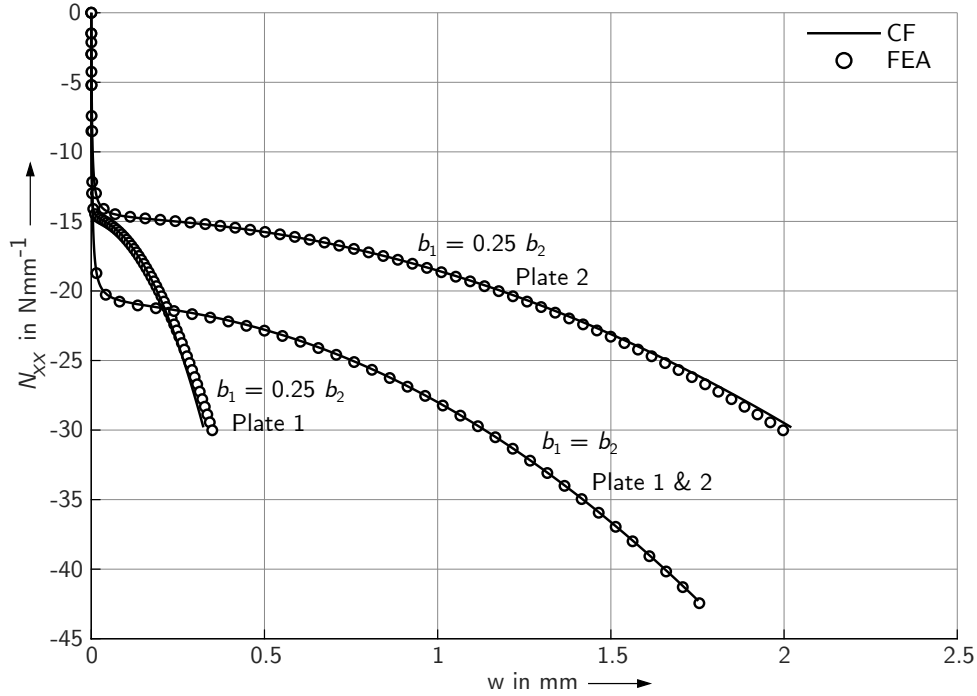


Figure 4: Imperfect stability behaviour for a two-plate assembly obtained by the present closed-form analytical method (CF) and plotted together with a FEA of the two-plate assembly; $w_i = 0.002$; lay-up $[0^\circ 90^\circ 0^\circ 90^\circ]_s$; $a = 500$ mm; $b_1 + b_2 = 300$ mm, $E_1 = 157000$ MPa; $E_2 = 8500$ MPa; $G_{12} = 4200$ MPa; $\nu_{12} = 0.35$; $t_{ply} = 0.184$ mm

- Excellent results are obtained for local buckling in case of a uniaxially compressed panel. Also, good agreement is achieved in case of shear loading. The postbuckling behaviour of the two-plate assembly is well predicted.
- Closed-form analytical approaches indicate that they offer the advantage to be highly efficient and can yield satisfactory approximate results for preliminary design.
- Computational efficiency comes with the loss of generality of the analytical model. For different boundary conditions and loadcases, the computational model needs to be individually derived.

5 ACKNOWLEDGEMENTS

The authors thank the German Research Foundation (DFG) for their financial support [project number 399128978].

REFERENCES

- [1] Jain, H. K. and Upadhyay, A. Buckling behavior of blade-, angle-, T-, and hat-stiffened FRP panels subjected to in-plane shear. *J. Reinf. Plast. Compos.* (2010) **29**:3614–3623.

- [2] Lamberti, L., Venkataraman, S., Haftka, R.T. and Johnson, T.F. Preliminary design optimization of stiffened panels using approximate analysis models. *Int. J. Numer. Methods Eng.* (2003) **57**:1351–1380
- [3] Schilling, J. C. and Mittelstedt, C. Local buckling analysis of omega-stringer-stiffened composite panels using a new closed-form analytical approximate solution. *Thin-Walled Struct.* (2020) **147**:106534
- [4] Schilling, J. C. and Mittelstedt, C. Shear-buckling of omega-stringer-stiffened panels. Submitted.
- [5] Mittelstedt, C. and Becker, W. *Strukturmechanik ebener Laminate*. Studienbereich Mechanik, Technische Universität Darmstadt (2016).
- [6] Vescovini, R. and Bisagni, C. Single-mode solution for post-buckling analysis of composite panels with elastic restraints loaded in compression. *Compos. B. Eng.* (2012) **43**:1258–1274
- [7] Beerhorst, M. *Entwicklung von hocheffizienten Berechnungsmethoden zur Beschreibung des Beul- und Nachbeulverhaltens von versteiften und unversteiften Flächentragwerken aus Faserverbundwerkstoffen*. Technische Universität Berlin, Ph.D. thesis (2014).
- [8] Reddy, J.N. *Mechanics of Laminated Composite Plates and Shells: Theory and Analysis*. CRC Press, second ed., (2004).
- [9] Jones, R.M. *Mechanics of Composite Materials*. Taylor & Francis, second ed., (1999).
- [10] Timoshenko, S. and Gere, J.M. *Theory of Elastic Stability*. Dover Publications, second ed. (2009).